Shell-isolated nanoparticle enhanced Raman spectroscopy (SHINERS) investigation of benzotriazole film formation on Cu(100), Cu(111), and Cu(Poly)

ARTICLE *in* JOURNAL OF RAMAN SPECTROSCOPY · JANUARY 2012

Impact Factor: 2.67 · DOI: 10.1002/jrs.2989

Research Article

Journal of RAMAN SPECTROSCOPY

Received: 13 December 2010 Accepted: 17 April 2011 Published online in Wiley Online Library: 19 May 2011

(wileyonlinelibrary.com) DOI 10.1002/jrs.2989

Shell-isolated nanoparticle enhanced Raman spectroscopy (SHINERS) investigation of benzotriazole film formation on Cu(100), Cu(111), and Cu(poly)

Nicole R. Honesty and Andrew A. Gewirth*

Benzotriazole (BTAH) is well known as an effective corrosion inhibitor for Cu because of its ability to make a coordination polymer film on the surface that provides a barrier to Cu oxidation. BTA^- film formation was investigated on single-crystal and polycrystalline Cu surfaces with shell-isolated nanoparticle enhanced Raman spectroscopy (SHINERS) using silica-encapsulated Au nanoparticles. Potential-dependent spectra display reversible film formation on polycrystalline Cu and irreversible film formation on single-crystal Cu. Grain boundaries leading to smaller BTA^--Cu oligomers are proposed to be the reason for cathodic degradation of the BTA^- polymeric films on polycrystalline Cu.

Supporting information may be found in the online version of this article.

Keywords: SERS; SHINERS; benzotriazole; copper

Introduction

Corrosion inhibition is important in processing metals submersed in oxidizing solutions. Benzotriazole (BTAH) is a common additive in polishing slurries and plating baths because of its ability to inhibit corrosion of Cu and its alloys.[1] The general understanding of the mechanism of inhibition gathered from Fourier transform infrared spectra[2,3] and surface-enhanced Raman scattering (SERS)[4–6] is that when Cu^+ ions are released from the surface, a coordination polymer of Cu(I) and BTA^- forms which prevents further oxidation. There is a facial dependence on the degree of corrosion inhibition in the order of (100) > (110) > (111).[7] In aqueous sulfuric acid solutions, scanning tunneling microscopy (STM)[8–10] studies have shown that a sulfate layer forms on the Cu surface that serves a template for BTA adsorption. The BTA layer on the Cu(100) face is highly ordered, whereas the BTA^- layer on Cu(111) is highly disordered. The disorder of the BTA film is attributed with decreased corrosion inhibition on the (111) face.

Reversible BTAH physisorption[11,12] is known to occur at concentrations below 0.17 mM which is the critical concentration for effective inhibition; however, the studies mentioned above use concentrations well above this concentration. Concentration of BTAH also affects the corrosion mechanism. When polycrystalline Cu electrodes are anodically polarized in NaCl solutions, intergranular corrosion occurs at low BTAH concentrations (1 mM) and pitting occurs at greater concentrations of BTAH.[13]

One major issue regarding the BTA^- film concerns the reversibility of its formation, especially at BTA concentrations above 0.17 mM. On this issue, infrared–visible sum frequency generation (SFG),[14] infrared reflection adsorption spectroscopy (IRRAS),[2] and quartz crystal microbalance (QCM)[15,16] measurements all agree that the BTA^- film formation is irreversible as a function of applied potential. Such is not the case with numerous SERS studies, obtained on polycrystalline Cu, which show reversible BTA^- film formation based on analysis of spectral features associated with the film.[4,6,17]

One reason why SERS measurements might show reversible behavior while those from IRRAS and SFG do not is that the SERS measurements are performed on polycrystalline materials while the former use single crystals. The use of single crystals in an SERS experiment is difficult, since the plasmon mode giving rise to the SERS signal is enhanced on a roughened surface. The roughened surface also raises issues regarding the origin of the SERS signal, as asperities ('hot spots') where the **E** field is high might behave differently from the rest of the surface. Recently, Tian reported an elegant way to study single-crystal surfaces, called SHINERS.[18,19] With SHINERS, the signal enhancement comes from silica-encapsulated gold particles deposited onto the surface of interest. The gold particles provide the enhancement, while the silica shell prevents agglomeration of the particles and direct interaction of the gold with the surface of interest. This eliminates the need for the surface to be SERS active and allows the direct investigation of single crystal electrodes.

In this article, we revisit BTA film formation to ascertain whether this process is reversible or irreversible in SERS measurements.

* *Correspondence to: Andrew A. Gewirth, Department of Chemistry, University of Illinois at Urbana-Champaign, 600 S. Mathews Avenue, Urbana, IL 61801, USA. E-mail: agewirth@illinois.edu*

Department of Chemistry, University of Illinois at Urbana-Champaign, Urbana, IL 61801, USA

Experimental

Chemicals were of reagent grade and used as received. All solutions were prepared using ultrapure water (Milli-Q UV plus, Millipore Inc., 18.2 MΩ cm) and H_2SO_4 (Ultrex II, J. T. Baker).

Silica-coated gold sols were synthesized as described,[18] but a brief description follows. A gold sol with 20 nm diameter particles was synthesized by using sodium citrate reduction. The particles were coated with (3-aminopropyl)trimethoxysilane (APS) and a ~1 nm film of silica on the gold particles was created by immersing the APS-coated particles in an aqueous solution containing 0.54 wt% sodium silicate that was left stirring for 2–3 days. Excess reagents and side products were removed by dialysis. Transmission electron microscopy (TEM) data were obtained with a Joel 2100 Cryo electron microscope operating at 200 kV. TEM grids were prepared by drop-casting 10 µl of purified gold nanoparticle solution on the TEM grids and drying them in air. Figure S1 (Supporting Information) shows TEM images of the particles, which are ~17 nm in diameter.

The working electrodes were 1 cm diameter Cu(111) and Cu(100) single crystals (Monocrystals Co.). Surface orientation of the crystals was verified by four-circle X-ray diffraction (XRD). Crystals were mechanically polished to a 0.25 µm grit size (Metadi Supreme diamond suspension, Buehler) and electropolished in 50% w/v phosphoric acid at 2 V *versus* a Pt counter electrode for 30 s. After electropolishing, the crystals were rinsed with Millipore water and dried under Ar. A film of SiO_2-coated gold particles was made by drop-casting 50 µl of the suspended particles onto the crystal and drying under Ar. Electrochemistry was performed using a CHI760C or CHI 760D potentiostat (CH Instruments) in a two-compartment glass cell with Au wire counter electrode separated from working electrode compartment by glass frit and a Ag/AgCl 'no-leak' (Cypress) reference electrode connected to the working electrode compartment by Luggin capillary. Polycrystalline Cu disks were also used as working electrodes. They were prepared as above except that the elecropolishing solution was 85% w/v phosphoric acid. For comparison, the polished disks were also electrochemically roughened as described by Chan and Weaver.[4]

Raman experiments were performed using an *in situ* cell described previously.[20] Potential control was maintained with a CV-27 potentiostat (BAS). The He–Ne laser ($\lambda = 632.8$ nm) was projected onto the sample at ~45° incidence. Scattered radiation was collected with an *f*/4 focusing lens and focused at the entrance slit of a monochromator. A 1200 grooves/mm grating dispersed the radiation onto a cooled charge coupled device (CCD, Andor). Typical acquisition time was 30 s.

Results and Discussion

Figure 1 shows the cyclic voltammograms of particle-coated single-crystal copper surfaces. The particle coating does not appear to affect the onset of hydrogen evolution or Cu dissolution in agreement with the literature.[8,10,21] In voltammetry, although there are minimal differences for the onset hydrogen evolution on different faces,[2,21] crystallographic orientation has no significant effect on the kinetics of Cu dissolution in BTAH-containing H_2SO_4 solutions.[8]

Representative Raman spectra from solid BTAH and an aqueous solution consisting of 0.75 mM BTAH + 0.1 M H_2SO_4 as well as SERS of Cu(poly) and SHINERS from Cu(111), Cu(100), and Cu(poly) immersed in the same solution are displayed in Fig. 2. These spectra

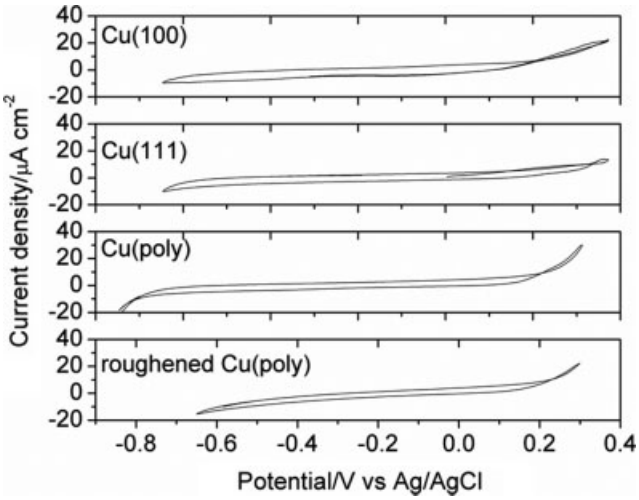

Figure 1. Cyclic voltammograms of particle-coated Cu(100), Cu(111), Cu(poly), and roughened Cu(poly) in 0.75 mM BTA, 0.1 M H_2SO_4 at 50 mV s^{-1} scan rate.

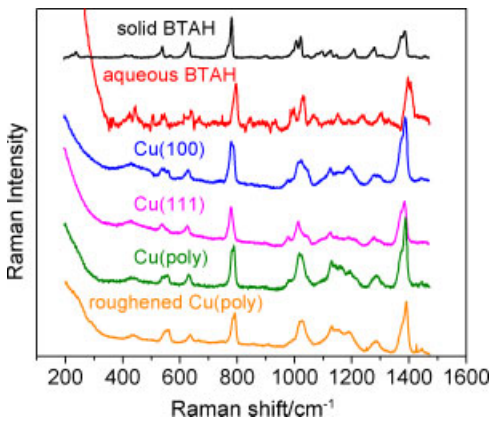

Figure 2. Raman spectrum of solid BTA; 0.75 mM BTA, 0.1 M H_2SO_4; and 0.75 mM BTA, 0.1 M H_2SO_4 on Cu (100) at −0.7 V *versus* Ag/AgCl, on Cu(111), on polycrystalline Cu, and on roughened polycrystalline Cu. Intensities are normalized to the 785 cm^{-1} mode.

display a number of peaks that match with those assigned by Chan and Weaver[4] (Table 1). Differences between the SERS obtained from the solid surfaces and aqueous and solid BTAH are similar to those described previously and are shown in Table 1.[4–6,17,22–24] The spectra obtained from single-crystal Cu strongly resemble that of polycrystalline Cu except for the relative intensity of the modes between 1100 and 1200 cm^{-1} and the breathing modes at 785 and 1390 cm^{-1}. Interestingly, the SERS obtained from the Cu(poly) surface without the silica-coated Au particles is identical to that from the Cu(poly) surface with the particles. This observation shows that the particles do not affect the BTAH Raman response.

Figure 3 shows the potential-dependent spectra obtained for all the four surfaces considered. The spectra display the same peaks for all surfaces at roughly the same energy and respond similarly to potential changes. As the potential is swept in the anodic direction, the 1020 and 1190 cm^{-1} modes increase in intensity relative to the neighboring peaks. This difference in intensity remains as the scan changes direction for the single-crystal faces but disappears for the polycrystalline Cu. For better comparison of the surfaces, Fig. S2 shows an overlay of the

Table 1. Peaks and their assignments for the spectra shown in Fig. 1

Solid BTA	Solution BTA	Cu(100)	Cu(111)	Cu(poly)	Roughened Cu(poly)	Chan and Weaver[4]	Band assignments[4]
Wavenumber (cm^{-1})							
235							Skeletal torsion
429		442	428	435	436	440	Skeletal torsion
537		545	537	549	553	555	Triazole ring bend
628		627	626	630	635	653	Triazole ring torsion
779	796	781	779	785	788	790	Benzene ring breathing
	993	978	976	982	974		SO_4 symmetric stretch
1006		1013	1014	1019		1010	Benzene skeletal and (CH) bend
1022	1030	1024		1025	1024	1020	Benzene skeletal and (CH) bend
1072		1045	1046				(NH) bend
1127		1129	1125	1128	1127		(CH) bend
1147		1134	1148	1134	1145	1140	(NH) bend[6]
1171		1158	1165	1164	1159	1160	Triazole asymmetric stretch and (NH) bend
1206		1189	1192	1193	1196	1190	Triazole ring breathing mode (C–C–C in-plane bending)[17]
1280		1285	1297	1286	1284	1286	Skeletal stretch (NH) bend and (CH) bend
1374		1373	1375	1377	1380	1370	Fermi resonance with 1385
1387	1396	1388	1388	1388	1391	1385	Combination breathing
		1443		1444		1440	Skeletal stretch

spectra obtained from the three surfaces considered here at three different potentials: the starting potential of −0.7 V, a potential where dissolution of Cu is prevalent at 0 V, and back to −0.7 V after the cathodic sweep. The spectra from the three surfaces are similar except for the differences in relative intensity in the 1100–1200 cm^{-1} region where three peaks have been assigned by Chan and Weaver: 1140 cm^{-1} which is a NH in-plane bending mode assigned by Youda *et al.*,[6] 1160 cm^{-1} associated with a combination of the asymmetric triazole stretching and NH bending modes, and 1190 cm^{-1} which is due to the triazole ring breathing C–C–C in-plane bending of BTA^-.[17] The 1140 cm^{-1} mode is typically associated only with surface-attached BTAH, while the 1190 cm^{-1} mode is associated with the BTA^- Cu film arising as a consequence of anodic oxidation of BTAH on Cu.[6,17]

When the potential is swept in the anodic direction, the 1190 cm^{-1} peak increases in intensity relative to the neighboring peaks for all three surfaces. As the potential is swept in the cathodic direction, the 1190 cm^{-1} peak continues to increase in intensity for the (111) and (100) faces but decreases for the polycrystalline face.

Figure 4 displays the relative peak intensity of the 1190 cm^{-1} mode *versus* that of the 1140 cm^{-1} mode. The 1190 cm^{-1} mode is associated with BTA^-, whereas the 1140 cm^{-1} mode is assigned to the NH bending mode of adsorbed BTAH. An increase in the 1190/1140 ratio is thus associated with growth of the BTA^- (Cu^I) film. Figure 4 shows that this ratio increases for both single-crystal surfaces from the start of potential scanning at −0.7 V to the anodic limit of the scan. The ratio stops increasing on the Cu(100) face at about −0.2 V and remains constant as the potential is swept in the cathodic direction. However, the ratio for Cu(111) continues to increase as the potential is swept in the cathodic direction until −0.3 V when it plateaus. The ratio for polycrystalline surface does not start increasing until −0.3 V, grows substantially until the anodic limit of the scan, remains stable as the potential is swept toward the negative limit, and then falls after −0.4 V to the initial value. Thus, all three surfaces (Cu(111), Cu(100), and Cu(poly)) exhibit different film growth behavior.

The behavior displayed in the SHINERS of the BTA^- film formed on single-crystal Cu here matches that found in other *in situ* studies using Cu single crystals. STM,[8,10] IRRAS,[2] and SFG[14] all show that the BTA^- film persists on the cathodic sweep, while film formation on the polycrystalline surface in sulfuric acid – as measured in SERS – is reversible.[4,6] Thus reversible BTA film formation observed in SERS on Cu seems to be intrinsic to the polycrystalline material used previously.[4,6]

Why should the SERS signal show reversibility of the film on polycrystalline Cu? There are several possible reasons. First, Cl^- – possibly introduced during roughening of the Cu surface – could change properties of the BTA^- film. Many studies have shown that adding Cl^-, which competes for surface sites and coordinates to the BTA^- – Cu film, will promote reversibility.[2,5,14,25] However, other SERS studies on polycrystalline Cu explicitly avoid roughening in Cl^--containing solution, yet the reversibility persists.[6] Additionally, the Cu(poly) surface covered with the particles in these measurements was not roughened and was not exposed to a Cl-containing solution, yet it too exhibited film growth reversibility. Second, the large number of grain boundaries present on the polycrystalline material might affect the BTA^- film. Calculations interrogating monomeric BTA^- and BTA^--Cu oligomer chains show that the BTA^--Cu chains adsorb more strongly to the Cu surface than monomeric BTA^-, thus allowing dissolution of the film from defect sites at grain boundaries.[26–28] Tian has suggested that negative potentials both reduce the size of the oligomers and attract sufficient H^+ to reprotonate coordi-

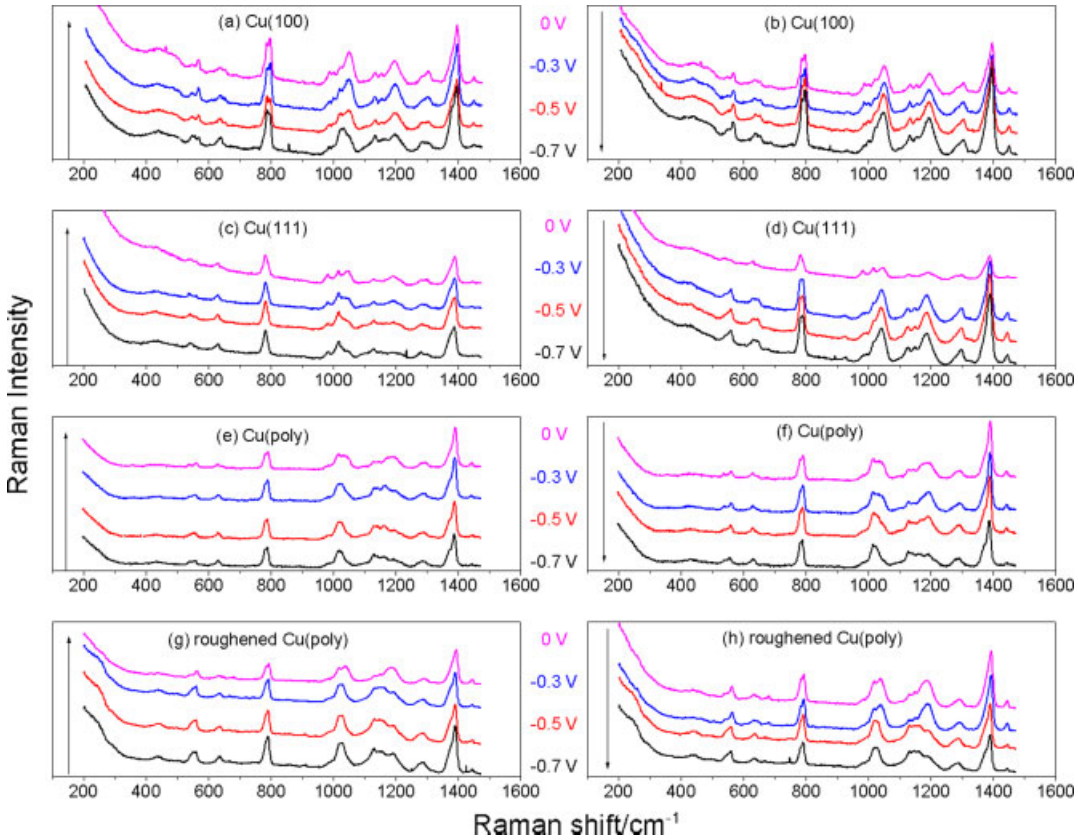

Figure 3. Potential-dependent spectra for Cu(100), Cu(111), and polycrystalline Cu in 0.75 mM BTA, 0.1 M H_2SO_4 for the anodic sweep (a), (c), (e), and (g) and the cathodic sweep (b), (d), (f), and (h). Spectra are offset for clarity. Arrows indicate scan direction.

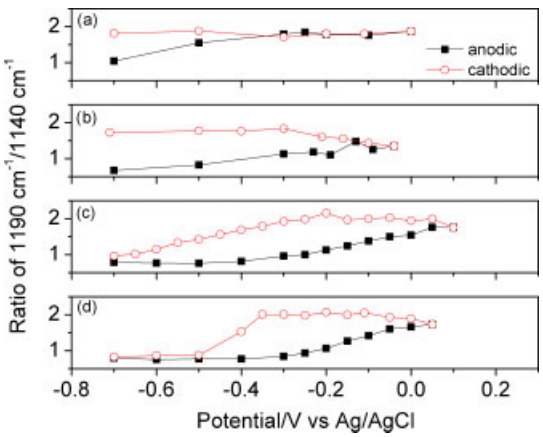

Figure 4. Potential-dependent ratio of peak intensities for 1190 cm^{-1}/1140 cm^{-1} bands for Cu(100) (a), Cu(111) (b), Cu(poly) (c), and roughened Cu(poly) (d) in 0.75 mM BTA, 0.1 M H_2SO_4.

nated BTA^-.[5,25] A similar mechanism is suggested to occur with BTA films with ionic liquids as the solvent.[29] Disruption at grain boundaries could allow reprotonation to occur on BTA^--Cu films formed on polycrystalline Cu.

The SHINERS procedure allows direct interrogation of both single-crystal and unroughened polycrystalline electrodes and provides results that correlate well with those from other techniques. With this understanding, interrogation of other processes at smooth electrode surfaces can proceed. In this study, we show that film formation depends on the face of the Cu crystal exposed as suggested from other measurements but was never shown directly using Raman spectroscopy. Polycrystalline surfaces exhibit reversible BTA^- film growth, likely due to the presence of grain boundaries that inhibit formation of larger and more irreversible oligomers.

Acknowledgements

This work was funded by the National Science Foundation. We thank Prof. Catherine J. Murphy and Stefano Boulos for synthesizing the silica-coated Au nanoparticles. We also thank Mauro Sardela for XRD measurements performed in the Frederick Seitz Materials Research Laboratory Central Facilities, University of Illinois, which is partially supported by the U.S. Department of Energy under Grants DE-FG02-07ER46453 and DE-FG02-07ER46471.

Supporting information

Supporting information may be found in the online version of this article.

References

[1] M. Finsgar, I. Milosev, *Corros. Sci.* **2010**, *52*, 2737.
[2] M. E. Biggin, A. A. Gewirth, *J. Electrochem. Soc.* **2001**, *148*, C339.
[3] G. W. Poling, *Corros. Sci.* **1970**, *10*, 359.
[4] H. Y. H. Chan, M. J. Weaver, *Langmuir* **1999**, *15*, 3348.
[5] J. Rubim, I. G. R. Gutz, O. Sala, W. J. Orville-Thomas, *J. Mol. Struct.* **1983**, *100*, 571.

[6] R. Youda, H. Nishihara, K. Aramaki, *Corros. Sci.* **1988**, *28*, 87.
[7] S. M. Mayanna, T. H. V. Setty, *Corros. Sci.* **1975**, *15*, 627.
[8] W. Polewska, M. R. Vogt, O. M. Magnussen, R. J. Behm, *J. Phys. Chem. B* **1999**, *103*, 10440.
[9] M. R. Vogt, A. Lachenwitzer, O. M. Magnussen, R. J. Behm, *Surf. Sci.* **1998**, *399*, 49.
[10] M. R. Vogt, W. Polewska, O. M. Magnussen, R. J. Behm, *J. Electrochem. Soc.* **1997**, *144*, L113.
[11] N. K. Allam, H. S. Hegazy, E. A. Ashour, *J. Electrochem. Soc.* **2010**, *157*, C174.
[12] C. Jin-Hua, L. Zhi-Cheng, C. Shu, N. Li-Hua, Y. Shou-Zhuo, *Electrochim. Acta* **1997**, *43*, 265.
[13] A. M. Abdullah, F. M. Al-Kharafi, B. G. Ateya, *Scr. Mater.* **2006**, *54*, 1673.
[14] Z. D. Schultz, M. E. Biggin, J. O. White, A. A. Gewirth, *Anal. Chem.* **2004**, *76*, 604.
[15] F. M. Al Kharafi, A. M. Abdullah, B. G. Ateya, *J. Appl. Electrochem.* **2007**, *37*, 1177.
[16] F. M. Bayoumi, A. M. Abdullah, B. Attia, *Mater. Corros.* **2008**, *59*, 691.
[17] R. Youda, H. Nishihara, K. Aramaki, *Electrochim. Acta* **1990**, *35*, 1011.
[18] J. F. Li, Y. F. Huang, Y. Ding, Z. L. Yang, S. B. Li, X. S. Zhou, F. R. Fan, W. Zhang, Z. Y. Zhou, Y. WuDe, B. Ren, Z. L. Wang, Z. Q. Tian, *Nature* **2010**, *464*, 392.
[19] D. Graham, *Angew. Chem., Int. Ed.* **2010**, *49*, 9325.
[20] M. E. Biggin, PhD Thesis, *In situ vibrational spectroscopic and electrochemical study of electrodeposition additives on copper surfaces*, University of Illinois at Urbana-Champaign (Champaign, IL), **2001**.
[21] Y. C. Wu, P. Zhang, H. W. Pickering, D. L. Allara, *J. Electrochem. Soc.* **1993**, *140*, 2791.
[22] D. W. Shoesmith, W. Lee, *Electrochim. Acta* **1977**, *22*, 1411.
[23] K. L. Stewart, J. Zhang, S. T. Li, P. W. Carter, A. A. Gewirth, *J. Electrochem. Soc.* **2007**, *154*, D57.
[24] K. T. Carron, G. Xue, M. L. Lewis, *Langmuir* **1991**, *7*, 2.
[25] P. G. Cao, J. L. Yao, J. W. Zheng, R. A. Gu, Z. Q. Tian, *Langmuir* **2002**, *18*, 100.
[26] A. Kokalj, S. Peljhan, M. Finšgar, I. Milošev, *J. Am. Chem. Soc.* **2010**, *132*, 16657.
[27] A. Kokalj, S. Peljhan, *Langmuir* **2010**, *26*, 14582.
[28] Y. Jiang, J. B. Adams, *Surf. Sci.* **2003**, *529*, 428.
[29] L. A. F. Costa, H. S. Breyer, J. C. Rubim, *Vib. Spectrosc.* **2010**, *54*, 103.